BIBECHANA
Vol. 23, No. 3, August 2026, 41-52

ISSN 2091-0762 (Print), 2382-5340 (Online)
Journal homepage: http://nepjol.info/index.php/BIBECHANA
Publisher:Dept. of Phys., Mahendra Morang A. M. Campus (Tribhuvan University)Biratnagar

Green iron oxide particles for sustainable arsenic removal from water

Kshama Parajuli[1*], Shushan Bhujel[1], Saroj Kumar Yadav[1], Rajesh Pandit[2], Situ Shrestha Pradhanang[2], Kusum Shrestha[3], Motee Lal Sharma[1], Rameshwar Adhikari[1,3]

[1]*Central Department of Chemistry, Tribhuvan University, Kirtipur, Nepal.*
[2]*Department of Chemistry, Tri-Chandra Multiple Campus, Tribhuvan University Kathmandu, Nepal.*
[3]*Research Center for Applied Science and Technology, Tribhuvan University, Kirtipur, Nepal.*

*Corresponding author: Email: kshamaparajuli@yahoo.com

Abstract

In many parts of the world, including Nepal, millions of people rely on arsenic–contaminated ground water for household purposes. According to World Health Organization (WHO), arsenic is a group 1 carcinogen. Exposure to arsenic-contaminated water over a long time through drinking water may pose a significant health risk to humans. Hence, due to its high toxicity and carcinogenicity, removing arsenic from drinking water is critical to prevent worldwide poisoning. Different techniques are available for arsenic removal, but adsorption of arsenic using iron oxide material is more attractive due to low cost, eco–friendliness, sustainability and high affinity of iron oxide particles towards arsenic. Herein, iron oxide particles (IOPs) were prepared using an aqueous extract of locally available Melastoma malabathricum (MM) leaf, which acts as a metal reductant as well as stabilizing agent and a ferric chloride hexahydrate ($FeCl_{3.6}H_2O$) aqueous solution as a metal precursor for the synthesis of iron oxide particles. Systematic characterization of the prepared IOPs was carried out by FTIR, XRD, SEM/EDX analysis, and pHpzc determination. FTIR spectrum of the IOPs showed a peak at 549 cm^{-1} corresponding to Fe–O stretching, while its XRD study indicated the amorphous nature of the synthesized IOPs. The EDX analysis confirmed the presence of Fe, O, and C atoms as major elements, and the point of zero charge (pHpzc) of the prepared material was determined to be 6.98. The batch adsorption study revealed a maximum As(V) removal efficiency of 93.03% at a pH value of 3. The adsorption data of As(V) onto IOPs were best fitted with the Langmuir isotherm model, yielding a maximum adsorption capacity (qmax) of 103.63 mg/g. Further, the synthesized IOPs showed 70.11% arsenic removal from real ground water containing 74.6 μg/L of arsenic. This study highlights the use of locally available plant leaves aqueous extract for an efficient production of low–cost, environmentally benign IOPs with promising applications in the remediation of arsenic-contaminated water.

Keywords
Green synthesis, iron oxide particles, arsenic, adsorption, polluted water.

Article information
Manuscript received: April May 13, 2026; Revised: June 23, 2026; Accepted: July 12, 2026
DOI: https://doi.org/10.3126/bibechana.v23i3.94442
This work is licensed under the Creative Commons CC BY-NC License. https://creativecommons.org/licenses/by-nc/4.0/

1 Introduction

Arsenic (As), a naturally occurring metalloid, has been extensively investigated owing to its complex and often problematic relationship with living organisms. Arsenic can be found in the environment due to both natural processes and anthropogenic practices [1, 2]. Though arsenic has four oxidation states: 0 (arsenic), +III (arsenite), +V (arsenate), and −III (arsine) [3], in water bodies, arsenic is usually found in the +V (arsenate) and +III (arsenite) oxidation states. Arsenite is usually found in groundwater (considering anaerobic conditions), whereas arsenate, the oxidized pentavalent form, is found in surface water (considering aerobic conditions). Millions people living in South Asia, including India, Bangladesh, Nepal, and Srilanka etc are affected by the arsenic-contaminated water [4]. Nepal's geography is divided into three major regions and the southeast part of it near the Indian border is known as Tarai region where many of its districts such as Sunsari, Siraha, Saptari, Dhanusha, Sarlahi, Bara, Rautahat, Nawalparasi, Rupandehi, Kapilbastu, Banke, Kailali, and Kanchanpur, have reported an elevated level of arsenic in groundwater and have become a significant cause of concern [5, 6]. Due to economic and technical reasons the maximum permissible limit of arsenic in drinking water is 50 μg/L as set by the government of Nepal, which is 5 times higher than the maximum permissible arsenic level in drinking water (10 μg/L) as recommended by the WHO [5, 7]. Prolonged exposure to elevated concentration of arsenic in water bodies may lead to numerous health issues such as dermatitis, cardiovascular problems, diabetes, chronic bronchitis, immune disorders, peripheral nephropathy, liver damage, renal failure, adverse reproductive outcomes, hematological effects, cancers etc. [1, 8]. Therefore sustainable and cost-effective removal of arsenic from contaminated water is essential. Different techniques, including oxidation/reduction, precipitation, coagulation, ion exchange, adsorption, reverse osmosis, and membrane filtration are widely used for the purification of contaminated water. However many of these technologies remain inaccessible in many developing countries due to their high cost, associated limitations such as sludge generation, limited selectiveness and operational complexities [7]. Among the available methods, adsorption is one of the suitable methods for purification of arsenic-contaminated water due to its eco-friendliness and cost-effectiveness, as well as selectiveness [9]. A wide range of adsorbents including biomass, metal-loaded biomass, geopolymer, and metal oxides, etc., have been applied for the arsenic removal from water [10]. Among metal oxides, bio-synthesized iron oxide particles (IOPs) have attracted considerable research interest owing to their ease of preparation, biocompatibility, scalability, non-toxic nature, inertness, and its occurrence in biological system such as magnetosomes and ferritin [11] as well as their affinity toward arsenic.

Iron oxide can be synthesized through chemical, physical, and green approaches. Notably, green synthesis using plant parts aqueous extract, has gained increasing popularity because of abundant availability plants materials and elimination of toxic reducing agents and capping agents, such as sodium borohydride, amino acids, hydrazine [12]. Different metabolites present in plant extract such as phenols, proteins, carbohydrates, vitamins, tannins, terpenoids, play a direct role in the synthesis of iron oxide particles. Here, plant extracts metabolites reduce metallic salts and stabilize particles formation by preventing aggregation. Furthermore, characteristics of green synthesized particles including morphology, composition, structure, shape, size are strongly influenced by the chemical composition of the extract [13]. A wide variety of plant extracts have been successfully employed in the production of metal oxide particles, including Cu, Co, Ag, Au, Pd, Pt, Zn, and Fe (Fe_2O_3, Fe_3O_4) [14, 15]. The present study utilizes aqueous leaf extract of locally available *Melastoma malabathricum* (MM) as a reducing agent for the synthesis of IOPs under ambient conditions and evaluates their potential application in the removal of arsenic from arsenic-contaminated water.

2 Materials and methods

2.1 Chemicals

Ferric chloride hexahydrate ($FeCl_3.6H_2O$), Sodium arsenate ($Na_2HAsO_4.7H_2O$), were from Loba Chemie Pvt. Ltd; NaOH, HCl were from Drug House Pvt. Ltd., India; Sulphuric acid (H_2SO_4) was from Merk Life Science Pvt. Ltd, Ammonium heptamolybdate [$(NH_4)6Mo_7O_{24}.4H_2O$], Hydrazine hydrate ($NH_2NH_2.H_2O$), Buffer tablets of pH 4, 7, 9.2, were from Qualigens Fine Chemicals, India. All chemicals were used without any further purification.

2.2 Plant collection and aqueous extract preparation

Fresh plant leaves were brought from Madyanepal Municipality–7, Salghari, Lamjung, Nepal, and identified as *Melastoma malabathricum L* according to National Herbarium and Plant Laboratory (NHPL), Lalitpur, Nepal. Dirt in the leaves was removed using distilled water, shed dried and its

powder was made using a mechanical mill. Then 1 gram of the powder was taken in a beaker containing 50 mL distilled water and then the content was heated at 80 °C for half an hour. After cooling the sample, filtered the sample to get the aqueous extract. The extract was kept in fridge at 4 °C for further application.

2.3 Green synthesis of iron oxide particles

Bhujel et al. in 2025 [16] synthesis protocol was applied for synthesis of IOPs. In brief, 0.1M ferric chloride hexahydrate ($FeCl_3.6H_2O$) aqueous solution was taken in a beaker and to this freshly prepared of MM leaf aqueous extract was transferred drop by drop from the burette with constantly stirring the reaction mixture for an hour using magnetic stirrer. When all the plant extract was added into the iron solution, the reaction mixture pH was adjusted to 11 by adding 1M NaOH solution. Immediately the colour of the reaction mixture was changed from light yellow to dark black indicating the production iron oxide particles. After ageing for 24 hrs, the dark black precipitate was collected by centrifugation, washed several times with distilled water then with ethanol. The black precipitate was oven dried at 120 °C for 12 hours and then kept in a container for further use. The experimental images are presented in the Figure 1.

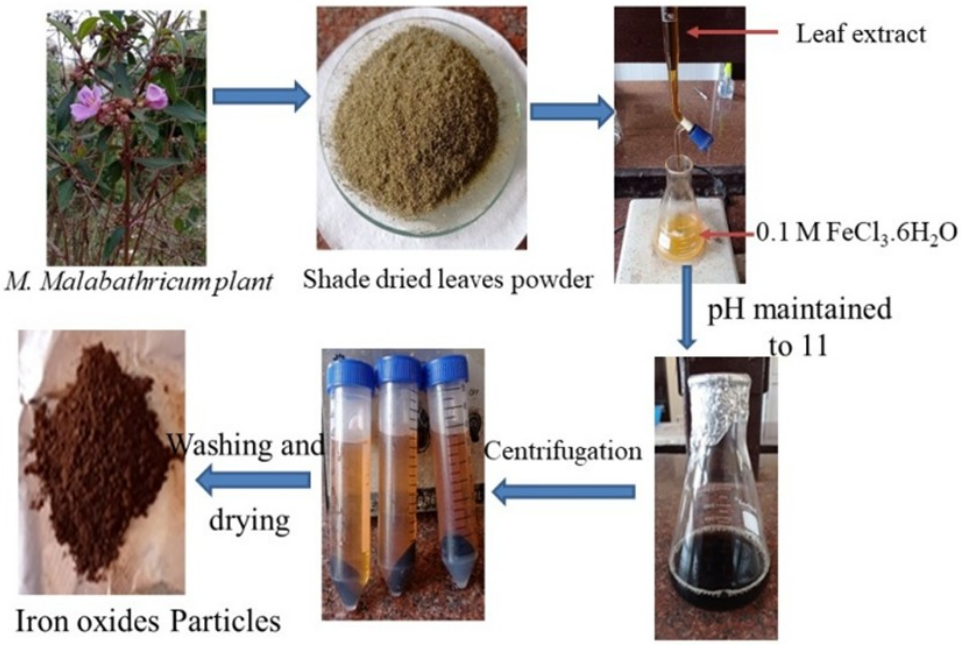

Figure 1: Photographs illustrating different stages of experimental procedures.

2.4 Characterization

FTIR analysis of samples was done using an IRAffinity–1s spectrophotometer (Shimadzu, Japan) over a wavelength range of 400–4000 cm^{-1} operated at a resolution of 2 cm^{-1}. The XRD study of the prepared IOPs was performed by using the Burker AXS-Diffractometer D_8 with Cu Kα radiation at the wavelength of 1.5405 Å. SEM/EDX study was done using Carl Zeiss Gemini, Germany, microscope and pH drift method was applied for the determination of pHpzc of the prepared sample using NaCl solution with concentrations of 0.01M, 0.05M, and 0.1M. Initial pH of the solutions was maintained at 1, 2, 3, 4, 5, 6, 7, 8, 9, and 10 using HCl and NaOH solutions. To the pH-maintained salt solution, 20 mg of synthesized IONP adsorbent was added and solutions were shaken for 24 hours. After filtering the equilibrated solutions, a pH meter was utilized to dictate the final pH of the filtrates. A plot was created by calculating the observed pH difference against the initial pH for all concentrations of NaCl solution. The point of intersection of the plot along the X-axis represents the point of zero charge of the material under study [17].

2.5 Batch adsorption performance of synthesized adsorbent as a function of pH

Batch adsorption experiments were performed to find out the effect of different parameters on adsorption process. Working As(V) solution of 5 mg/L was made from 1000 mg/L As(V) stock solution by serial dilution. The effect of the solution pH was

evaluated by shaking 25 mL As(V) working solution at different initial pH values ranging from 1–11 and taking 20 mg of the synthesized adsorbent in a reagent bottle shaking at a 200 rpm for 24 hours in a shaker. After 24 hours, the supernatants were filtered by Whatman filter paper No. 41 and the residual arsenic concentrate in the filtrate was determined by using the molybdenum blue spectrophotometric approach [17]. Equation (1) is used to compute the amount of adsorbate adsorbed per unit mass (q) of the adsorbent.

$$q = \frac{C_i - C_e}{W} \times V \tag{1}$$

where C_i = initial strength (in mg/L) of adsorbate before adsorption, C_e = equilibrium strength (in mg/L) of adsorbate after adsorption, V = volume of adsorbate solution taken (in L), and W = weight of adsorbent taken (in g).

Similarly, Equation (2) was employed to evaluate the % adsorption (% A) of the adsorbate onto the adsorbent.

$$\%A = \frac{C_i - C_e}{C_i} \times 100 \tag{2}$$

2.6 Adsorption isotherm study

A range of starting As (V) ion concentrations, from 5 ppm to 400 ppm were used in the adsorption isotherm investigation. 20 mg of adsorbents were placed in several clean, dried stopper bottles, and 25 mL of optimal pH-adjusted As(V) solution in varying concentrations was added to each bottle separately. Using the molybdenum blue spectrophotometric method, the concentrations of As(V) ions before and after adsorption were measured after the solution had been equilibrated for 24 hours. Freundlich adsorption isotherm (3), Langmuir adsorption isotherm (4), and Temkin isotherm (5) models were utilized to illustrate the adsorption behavior of As (V) onto synthesized IOPs.

2.7 Application of IOPs to eliminate arsenic from groundwater sample

Six groundwater samples were collected randomly from tube wells located in the Nawalparasi (West of Brdaghat Susta), Lumbini Province, Nepal, around Ramgram Municipality office, ward no. 12. The water hand pumps were nicely flushed (pumped out water for about 2 min) prior to collecting the sample. Then 1 L of water was collected in a plastic bottle from each spot. The 'Rapid Arsenic Test Kit for water analysis, QuickTM', developed by Industrial Test Systems, Inc. was chosen to conduct an initial test for arsenic. This rapid arsenic test showed that water sample no. 2 contained the highest level of arsenic among the 6 water samples. So water sample no.2 was used further to carry out arsenic removal test by the Atomic Absorption Spectroscopy (AAS) method. In this study, 20 mL of water from sample no. 2 was taken in six reagent bottles. Then 4, 6, 8, 10, 12, and 14 mg of synthesized IOPs were added to these reagent bottles, respectively and these reagent bottles were agitated at 210 rpm in a mechanical shaker for 24 hours. The mixture of reagent bottles was kept to settle down the adsorbent for 30 minutes. Then, Whatman No. 41 filter paper was employed to filter the content and the filtrate was collected in a separate clean plastic bottle and submitted to a commercial laboratory for the estimation of As before and after adsorption via (AAS)/Hydride generation system. Further, the quantitative analysis of other physicochemical parameters in the collected natural groundwater samples was also carried out following standard method.

3 Results and discussion

3.1 Characterization of the prepared IOPs

3.1.1 Point of zero charge (pHpzc)

In surface science, the point of zero charge of the material, or pHpzc, is crucial because it represents the pH when there is no charge on the adsorbent surface [18]. The pH drift procedure is a pH–affecting phenomenon and is one of the better methods for figuring out the point of zero charge of a material by utilizing different molar concentrations of NaCl. In this study, the synthesized IOPs were discovered to have a point of zero charges of 6.98 (Figure 2), indicating that at pH 6.98, the synthesized IOPs net charge is equal to zero. Thus, the prepared IOPs surface was negatively charged above pH 6.98 and positively charged below pH 6.98 [19].

3.1.2 FTIR study

The FTIR analysis (Figure 3) was performed to identify the possible functional groups present in the synthesized IOPs. Some distinct absorption bands seen in the FTIR spectrum are 3260, 2972, 2375, 2309, 1638, 1393, 1089 and 540 cm^{-1}. The board absorption band centered at 3260 cm^{-1} could be attributed to the stretching of OH group probably from polyphenols, flavonoids or terpenoids present in the plant extract while the band around 2972 cm^{-1} is probably due to the asymmetric

stretching of C-H bonds [20]. The peak at 1638 cm^{-1} is due C=C stretching vibration present on the aromatic ring [21]. Similarly the peak centered at 1392 is due to C-H starching of amide and 1089 cm^{-1} may be exhibited by C-O stretching present in the alcohols, carboxylic acids, ester and, ether groups etc of plant extract attached to the synthesized IOPs [22]. A band appeared at 2374 and 2309 cm^{-1} are may be due to the asymmetric stretching vibration of adsorbed atmospheric CO_2. The band at 549 cm^{-1} is due to the stretching vibration of Fe–O bonds in synthesized IOPs [23].

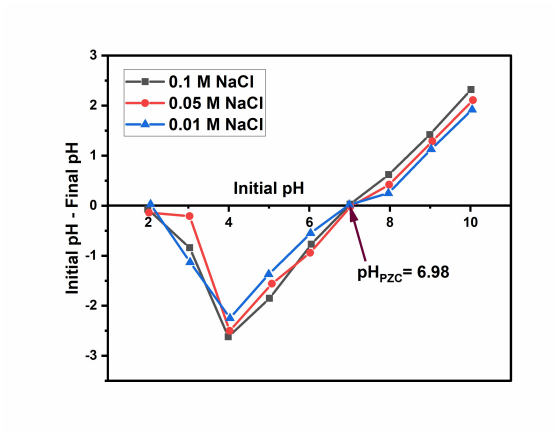

Figure 2: A plot of ΔpH (initial pH–final pH) against initial pH for determination point of zero charge pHpzc of synthesized IOPs.

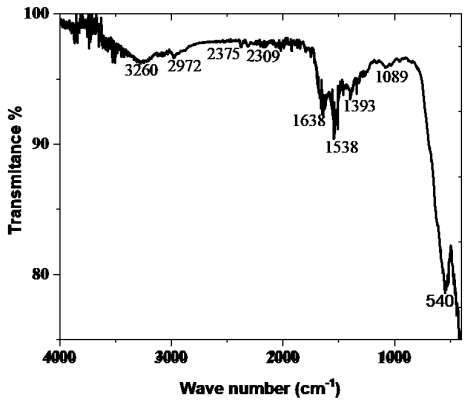

Figure 3: FTIR spectrum of the synthesized IOPs.

3.1.3 XRD study

The observed XRD pattern of the prepared IOPs is given in Figure 4. Since no distinct peaks in the XRD pattern are observed, it infers that the prepared IOPs are of amorphous nature [24,25]. However, very low intensity peaks centered at 2θ values of 35.23° and 63.2° could be due to the magnetite phase of iron oxide [26].

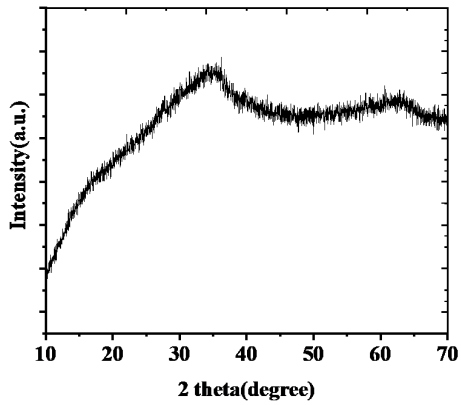

Figure 4: XRD pattern of the prepared IOPs.

3.1.4 SEM/EDX analysis

The SEM micrograph of the IOPs is shown in the Figure 5(a). In the image, the particles seem to be highly agglomerated, inhomogeneous, possessing rough surfaces, cracks and holes in them, underscoring the potential the adsorption capacity of the synthesized materials. High agglomeration of smaller particles is probably due to high surface energy and magnetic nature of the prepared IOPs. Similar agglomerated particles are reported by previous studies [17]. The elemental analysis of the sample was done by Energy Dispersive Spectroscopy (EDS) and major elements were found to be Fe (66.1%), O ((26.5%), C(4%) (Figure 5(b)), suggesting the compound formed were IOPs. The carbon presence in the sample can be attributed to application of plant extract while synthesizing material [16].

3.2 Batch adsorption study

3.2.1 Effect of initial pH of the adsorbate solution onto prepared adsorbent

Many factors, such as the surface charge of an adsorbent material, the type of metal to be adsorbed, and the chemistry of the adsorbent's functional group, are influenced by pH of the solution and therefore the adsorption process. The effect of solution pH on the removal% of As(V) by the synthesized adsorbent is shown in Figure 6 at an initial concentration of 5 ppm As(V) solution at room temperature. As can be seen, about 60% removal of arsenate was obtained at pH = 1 and on increasing pH, the percentage of removal was found to be increased and achieved maximum adsorption of 93.03% at pH 3. On further increase in pH, a gradual decrease in % adsorption of arsenate was obtained. Different adsorption behavior of arsenate

at different pH might be due to the existence of different forms of arsenate species as a function of initial pH of solution. Arsenate, can exist in different forms as a function of pH of the solution as H_3AsO_4 at pH<2, pH), $H_2AsO_4^{\breve{}}$ at pH = 2–7, $HAsO_4^{2\breve{}}$ at pH = (7–11.5), and AsO_4^{3-}t pH >11.5 [27].

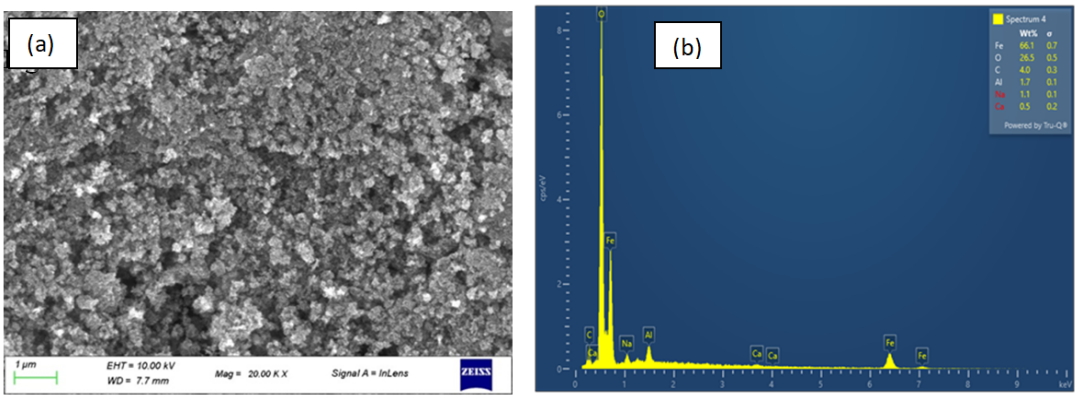

Figure 5: (a) SEM image, and (b) EDX spectrum of the prepred IOPs.

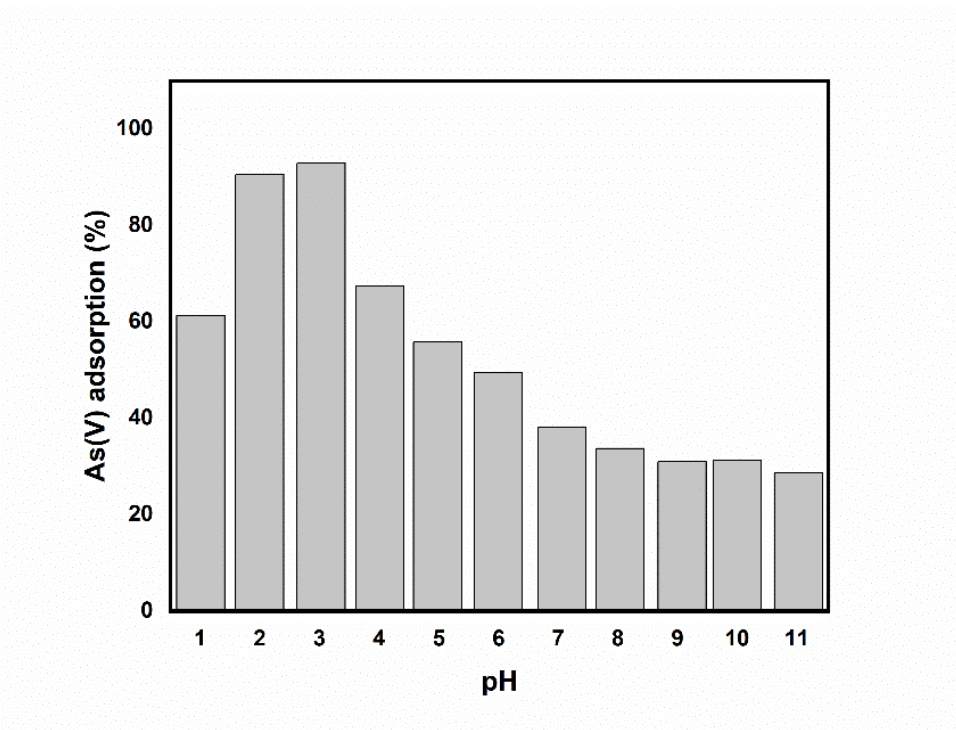

Figure 6: Effect of solution pH on the adsorption of As(V) onto synthesized IOPs.

At very low pH, i.e. at pH=1, there was low removal percentage of arsenate probably due to the weak interaction that occurs between the highly protonated adsorbent surface and uncharged arsenate molecule since it mainly exists in the form of neutral H_3AsO_4 molecule in this pH. While at pH=3, there was enhanced in % adsorption of arsenate because of increased in electrostatic attraction of positively charged adsorbent surface and negatively charged adsorbate as arsenate will remain in the $H_2AsO_4^{\breve{}}$ (2–7 pH), Further, the gradual decrease in removal % was observed as the initial pH was raised from 3 to 7 due to constantly decrease in the protonation degree of adsorbing species, causing a continuous weaken of electrostatic interaction between less positively charged surface of adsorbate and oxyanions of arsenic. While in alkaline pH i.e. pH $\geq$ 8, there was further decreased in adsorption % due increased concentration of OH^-, which may compete with anions of arsenic i.e. $HAsO_4^{2-}$ or AsO_4^{3-} [28]. In addition, the pH zero point charge (pHzpc) of prepared particles in this study was found to be 6.98 at room

temperature by pH drift method at pH range from 1 to 12, as presented in Figure 2. Hence, prepared adsorbent materials were positively charged between pH (1 to 6.98), while they were negatively charged in the pH $\geq$ 6.98 suggesting that prepared materials are more suitable for arsenate removal at acidic pH rather than basic pH solution. This clearly supporting our observed result of declining trend of adsorption at higher pH values which was partly caused by an increased electrostatic repulsion between the As(V) anion and the negatively charged particle surface.

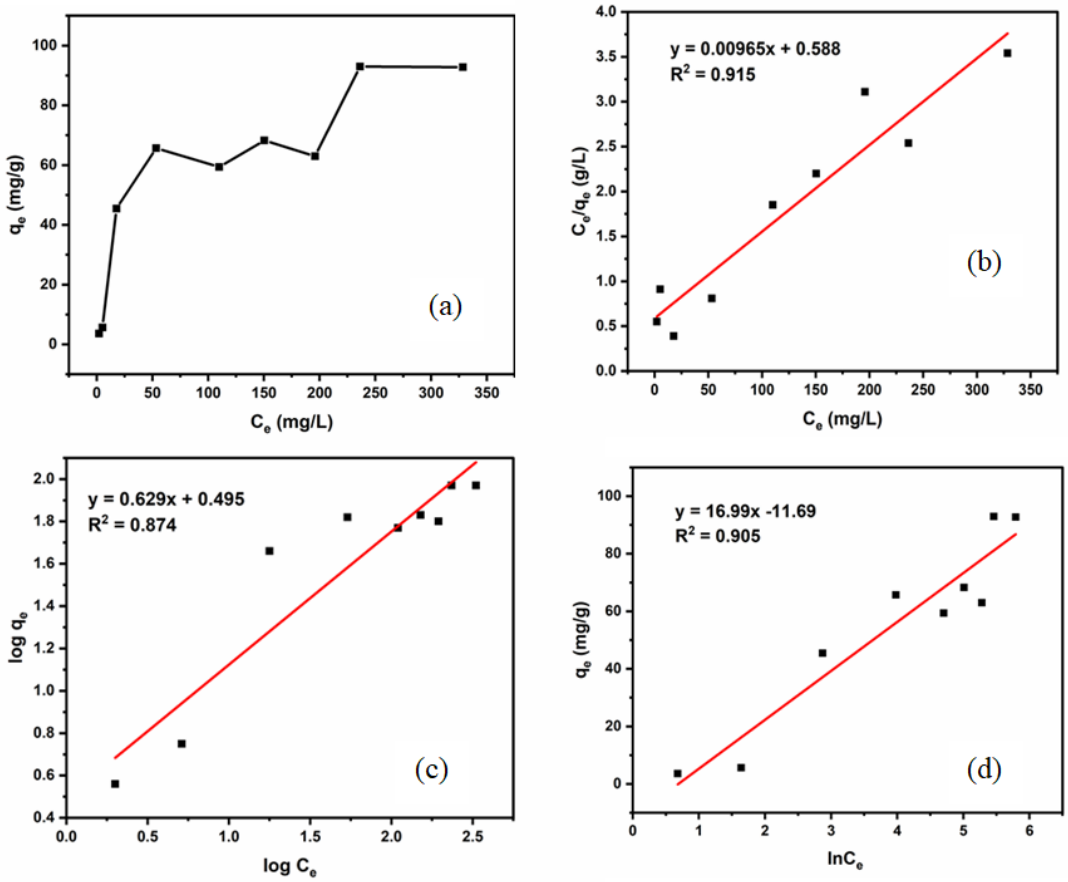

Figure 7: (a) A plot of qe versus Ce for different initial concentration of adsorbate (b) Langmuir isotherm plot (c) Freundlich isotherm plot (d) Temkin isotherm plot for adsorption of As(V) onto prepared adsorbent (IOP)s.

3.2.2 Effect of initial As(V) concentration

The removal effect of IOPs was evaluated at different initial concentrations as described above in section 2.6. As the initial strength of metal ions in aqueous solution increased, the adsorption amount increased as well until it reached a plateau and approached the equilibrium at a higher concentration, as shown in the Figure 7(a). The adsorption ability of the synthesized IOPs adsorbent rose from 3.63 to 92.96 mg/g when the starting concentration of As(V) was raised from 4.41 to 390.28 mg/L. Higher adsorption would come from the increased mass transfer driving force caused by a rise in As(V) concentration. This would also enhance the rate at which As(V) ions move from the bulk solution to the particle surface. Similar nature of results has been reported by several previous studies [29, 30].

In addition, linearized Freundlich adsorption isotherm (Equation (3)), Langmuir adsorption isotherm (Equation (4)), and Temkin isotherm (Equation (5)) modeling were performed using the cured experimental data to illustrate the adsorption behavior of As(V) onto synthesized IOPs.

$$\log q_e = \log K_f + \frac{1}{n} \log C_e \tag{3}$$

$$\frac{C_e}{q_e} = \frac{1}{q_{max}} C_e + \frac{1}{q_{max} K_L} \tag{4}$$

$$q_e = \frac{RT}{b_T} \ln A + \frac{RT}{b_T} \ln C_e \quad (5)$$

where C_e denotes the adsorbate concentration in mg/L after equilibrium. The value of qe is expressed in mg/g which denotes the quantity of adsorbate per unit mass of the adsorbent at equilibrium. The q_{max} represents the maximum adsorption capacity, measured in mg/g. K_L denotes the Langmuir equilibrium constant measured in L/mg [30]. The straight line is obtained after plotting C_e/q_e versus C_e and its slope and intercept are equal to $1/q_{max}$ and $1/(q_{max}.K_L)$ respectively, from which, we determined q_{max} and K_L. Similarly, A represents the Temkin isotherm constant (L/g) or equilibrium binding energy, R = 8.314 J/(mol.K) denotes the ideal gas constant, T represents the temperature in Kelvin (K), and b_T denotes the Temkin constant (J/mol). The linear plots were obtained in all models (see Figure 7(b, c, d) but the Langmuir model's linear plot fit the experimental data more closely, as shown by the correlation coefficient (R^2), indicating the homogenous distribution of active sites and adsorption limited to monolayer only [31]. Further, various parameters extracted from isotherm modeling study are presented in the Table 1.

Table 1: Parameters obtained from different isotherm models for As(V) adsorption

Parameter	Langmuir isotherm	Freundlich isotherm	Temkin isotherm
K_L (L/mg)	0.016	–	–
$q_{\max}$ (mg/g)	103.63	–	–
R^2	0.915	–	–
n	–	1.59	–
K_f (L/g)	–	3.13	–
R^2	–	0.874	–
b_T (J/mol)	–	–	147.29
A (L/g)	–	–	0.50
R^2	–	–	0.905

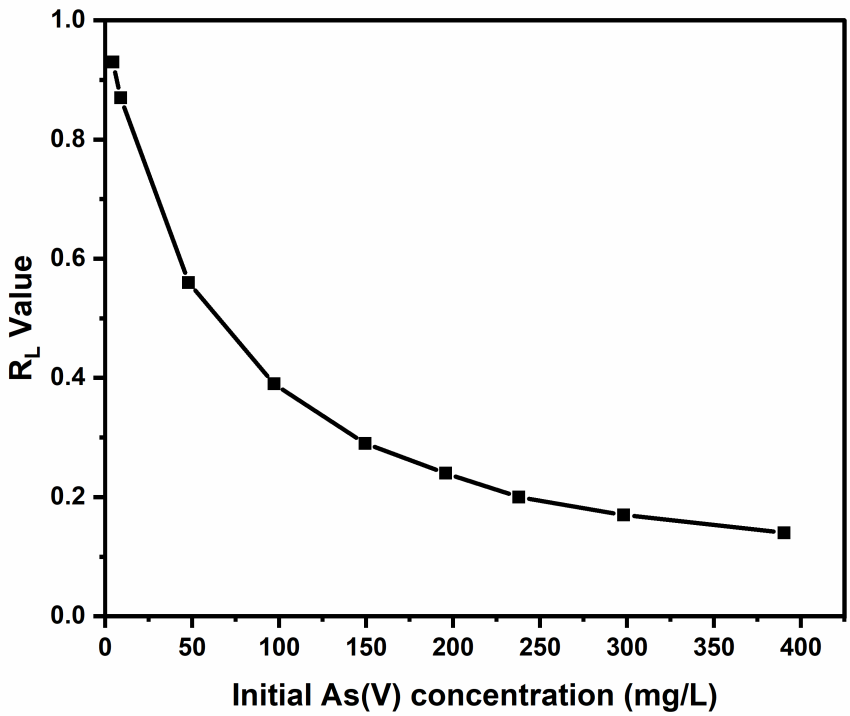

Figure 8: Plot of R_L value versus initial concentrations of As(V).

According to Hall et al. [32], the separation factor is used to evaluate whether the adsorption process is favourable or not. The separation factor is also known as the equilibrium parameter denoted by R_L is evaluated as given by Equation 6.

$$R_L = \frac{1}{1 + K_L C_i} \tag{6}$$

The calculated value of separation factor R_L values was plotted against the initial concentration of As(V) as displayed in Figure 8. All the evaluated values of R_L were between 0 to 1, which indicates a highly favorable adsorption process [33].

3.2.3 Comparison of adsorption capacity

The synthesized IOP's maximum adsorption capacity for As(V) along with a few other already investigated adsorbents by other researchers is tabulated in Table 2 for comparison. The synthesized IOPs exhibited a maximum adsorption capacity (q_{max}) of 103.63 mg/g, as evaluated from the slope of linear plot of Langmuir isotherm.

From the comparative studies with previous research, synthesized IOPs in this study showed a promising adsorption capacity for As(V). So the prepared IOPs could be an effective potential material for the elimination of As(V) from contaminated water.

Table 2: Comparison of IOPs with other adsorbents for As(V) adsorption capacity

S.N.	Name of adsorbent	Optimum pH	$q_{\max}$ (mg/g)	Reference
1	α-Fe_2O_3 nanostructure	3	51	[12]
2	α-Fe_2O_3 nanoparticles	3	47	[31]
3	Magnetite nanoparticles	2	62.89	[17]
4	Magnetic iron oxide nanoparticles	7	153.8	[34]
5	Zr(IV) loaded SOJR	3.1	74.42	[35]
6	IOPs	3	103.63	Present study

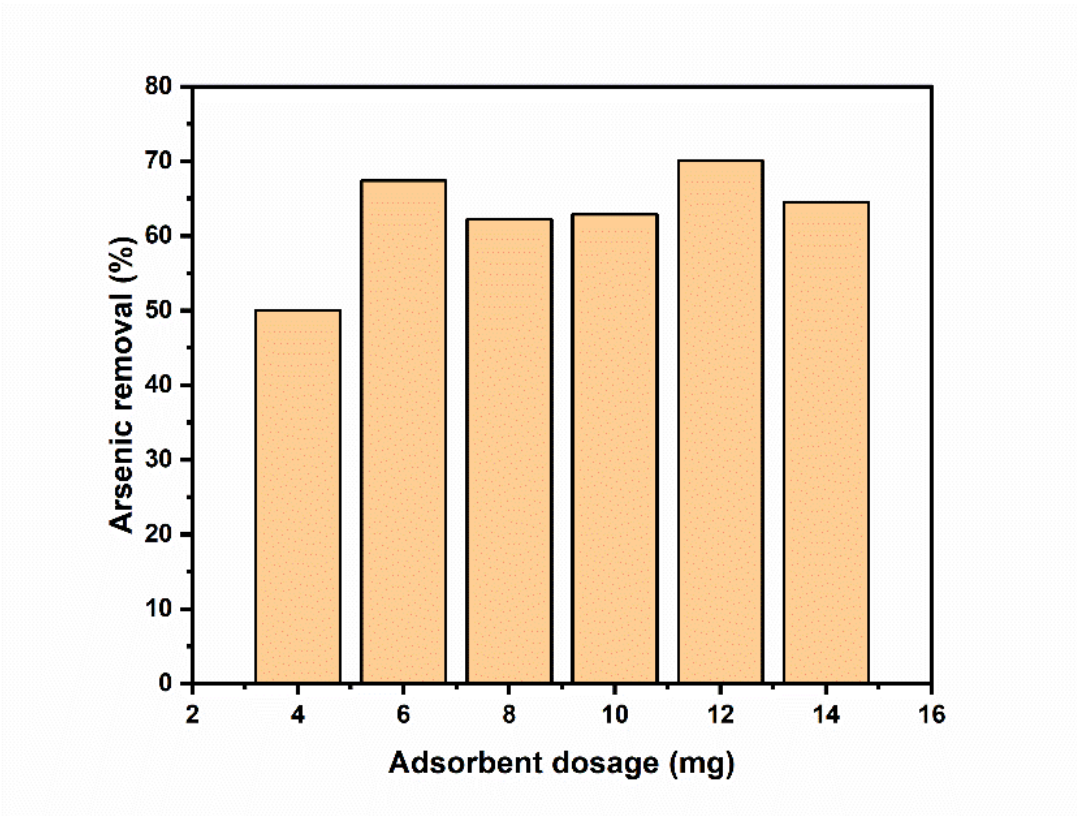

Figure 9: Arsenic removal of real water sample by different adsorbent dosages.

3.2.4 Practical application of the prepared IOPs

The applicability of the prepared IOPs for the removal of arsenic ion in a natural water sample was also carried out. For this, the arsenic-contaminated water samples were collected from Ramgram Municipality-12, Nawalparasi, Nepal and these water samples were analyzed by AAS technique. The initial concentration of arsenic in the water sample was found to be 74.60 μg/L, which is around 7.46 and 1.49 times higher than the WHO and Nepalese guidelines values respectively. The arsenic removal percentage depending on adsorbent (IOPs) dosages is shown in Figure 9. This experiment showed that 70.11 % of arsenic is removed by the adsorbent (synthesized IOPs) at the dosage of 12 mg. The concentration of arsenic was reduced from a starting concentration of 74.6 μg/L to a final concentration of 22.3 μg/L after mixing with 12 mg of synthesized IOPs.

In this study, the synthesized IOPs (4 mg in 20 mL water) or IOPs dosage of 0.2 g/L successfully minimized the arsenic level from the natural groundwater sample lower than the Nepalese drinking water standard (50 μg/L). Further, the tested natural groundwater sample was found to contain various co-existing ions such as carbonate (306.28 mg/L), chloride (10.47 mg/L), nitrate (35.5 mg/L), phosphate (8.36 mg/L), sulphate (15.22 mg/L), calcium (19.2 mg/L), iron (0.54 mg/L), and fluoride (0.63 mg/L) and hence many of these ions might alter the adsorption of arsenic from water [36]. In addition, on increasing the adsorbent dosage, the arsenic removal was increased as reported by early studies [30, 36]. Therefore, it is expected that increasing adsorbent dosage could enhance the removal of arsenic from real water samples as well.

4 Conclusion

Locally available *Melastoma malabathricum* (MM) leaves' aqueous extract was effectively utilized for synthesis of IOPs. The extract contributed as a reducing agent during the synthesis process replacing the toxic reagents that is otherwise needed for the reduction of the soluble salt used. The Fourier Transform Infrared Spectroscopy (FTIR) exhibited a characteristic absorption peak at 549 cm^{-1}, which corresponds to Fe–O stretching vibrations. The X-ray Diffraction (XRD) analysis confirmed that the synthesized iron oxide particles were predominantly amorphous in nature. Scanning Electron Microscopy (SEM) revealed that the particles possessed irregular morphologies with heterogeneous sizes, rough surfaces texture and agglomerated. The Energy Dispersive X–ray spectroscopy (EDX) further validated the elemental composition confirming the existence of Fe and O atoms in the prepared IOPs. The point of zero charge (pHpzc) of IOPs was determined to be 6.98 using pH drift method.

The batch adsorption experiments demonstrated that As(V) adsorption onto IOPs achieved a maximum adsorption capacity of 93.03 % at pH 3 at an adsorbent dosage of 0.8 g/L. The adsorption data were best fitted to Langmuir isotherm model yielding a maximum capacity (qmax) of 103.63 mg/g. Atomic Absorption Spectroscopy (AAS) of a natural arsenic-contaminated water sample collected from Ramgram Municipality-12, Nawalparsi, Nepal revealed an initial concentration of 74.6 μg/L, and the application of synthesized IOPs at the dosage of 0.6 g/L resulted in 70.11% of arsenic removal from the sample. These findings highlight the effectiveness of IOPs prepared using locally available MM plant leaf extract as a promising low-cost adsorbent for the remediation of arsenic contaminated water.

Acknowledgments

Authors are thankful to Assistant Prof. Dr. Santosh Khanal, Central Department of Chemistry, T.U., Kritipur, Kathmandu for SEM/EDX analysis and the respective department for providing the working space.

Conflicts of interest

The authors declare no conflicts of interest associated with the publication of this research paper.

Authors' contributions

KP, MLS and RA: Conceptualization, methodology, investigation, validation, formal analysis, review and editing. SB: Data curation, visualization, writing original draft. RP, SSP, SKY, KS: Reviewing and editing. All authors have read and agreed to the published version of the manuscript.

References

[1] Ng JC. Environmental contamination of arsenic and its toxicological impact on humans. Environmental Chemistry. 2005;2(3):146-60.

[2] Karimi P, Javanshir S, Sayadi MH, Arabyarmohammadi H. Arsenic removal from mining effluents using plant-mediated, green-synthesized iron nanoparticles. Processes. 2019;7(10):759.

[3] Sadee BA, Zebari SM, Galali Y, Saleem MF. A review on arsenic contamination in drinking water: sources, health impacts, and remediation approaches. RSC advances. 2025;15(4):2684-703.

[4] Aryan Y, Pon T, Panneerselvam B, Dikshit AK. A comprehensive review of human health risks of arsenic and fluoride contamination of groundwater in the South Asia region. Journal of water and health. 2024;22(2):235-67.

[5] Thakur JK, Thakur RK, Ramanathan AL, Kumar M, Singh SK. Arsenic contamination of groundwater in Nepal—an overview. Water. 2010;3(1):1-20.

[6] Rasaili P, Rai S, Sachin K, Saha B, Bhattarai A. Arsenic contamination of groundwater sources and a comparative study of its remediation by various conventional and recent approaches in Nepal. Vietnam Journal of Chemistry. 2024;62(3):281-95.

[7] Majumder A, Ramrakhiani L, Mukherjee D, Mishra U, Halder A, Mandal AK, et al. Green synthesis of iron oxide nanoparticles for arsenic remediation in water and sludge utilization. Clean Technologies and Environmental Policy. 2019;21(4):795-813.

[8] Du B, Wang Y, Li Y, Zhao X. Solvent-free fabrication of coral-like iron oxide nanoparticles from iron-bearing solid waste for the treatment of arsenic-containing wastewater: Synthesis process, adsorption mechanisms and DFT study. Separation and Purification Technology. 2026:137028.

[9] Moskalenko F, Garcia-Garcia A, Navarrete Á, Segura R, Liendo F, Roa V, et al. Fe_2O_3 and Fe_2O_3-Pd Nanohybrids for Arsenic Removal: Adsorption of As (III) and As (V) from Water and Mine Tailings. Journal of Hazardous Materials Advances. 2026:101044.

[10] Elmakki MAE, Ghosh S, Motente M, Ajiboye TO, Venter J, Adetunji AI. The Removal of Arsenic from Contaminated Water: A Critical Review of Adsorbent Materials from Agricultural Wastes to Advanced Metal–Organic Frameworks. Minerals. 2025;15(10):1037.

[11] Gao L. Enzyme-like property (nanozyme) of iron oxide nanoparticles. In: Iron oxide nanoparticles. intechopen; 2022. .

[12] Cao CY, Qu J, Yan WS, Zhu JF, Wu ZY, Song WG. Low-cost synthesis of flowerlike α-Fe_2O_3 nanostructures for heavy metal ion removal: adsorption property and mechanism. Langmuir. 2012;28(9):4573-9.

[13] Priya, Naveen, Kaur K, Sidhu AK. Green synthesis: An eco-friendly route for the synthesis of iron oxide nanoparticles. Frontiers in Nanotechnology. 2021;3:655062.

[14] Abuzeid HM, Julien CM, Zhu L, Hashem AM. Green synthesis of nanoparticles and their energy storage, environmental, and biomedical applications. Crystals. 2023;13(11):1576.

[15] Karunakaran G, Sudha KG, Ali S, Cho EB. Biosynthesis of nanoparticles from various biological sources and its biomedical applications. Molecules. 2023;28(11):4527.

[16] Bhujel S, Koju S, Yadav SK, Khadka D, Sharma ML, Parajuli K. Green Synthesis of Iron Oxide Nanoparticles Using Melastoma malabathricum Leaf Extract for Photocatalytic Degradation of Methylene Blue and Antibacterial Activity. Journal of Nanotechnology. 2025;2025(1):7616178.

[17] Parajuli K, Sah AK, Paudyal H. Green synthesis of magnetite nanoparticles using aqueous leaves extracts of Azadirachta indica and its application for the removal of As (V) from water. Green and Sustainable Chemistry. 2020;10(04):117-32.

[18] Parajuli K, Gautam B, Maharjan BL, Chhetri GG. Natural udroxyapatite as an adsorbent for microorganisms (MOS) from aqueous system. Scientific Study & Research Chemistry & Chemical Engineering, Biotechnology, Food Industry. 2023;24(3):233-47.

[19] Anirudhan TS, Unnithan MR. Arsenic (V) removal from aqueous solutions using an anion exchanger derived from coconut coir pith and its recovery. Chemosphere. 2007;66(1):60-6.

[20] Tran HN, You SJ, Chao HP. Effect of pyrolysis temperatures and times on the adsorption of cadmium onto orange peel derived biochar. Waste Management & Research. 2016;34(2):129-38.

[21] Basavegowda N, Mishra K, Lee YR. Synthesis, characterization, and catalytic applications of hematite (α-Fe_2O-3) nanoparticles as reusable nanocatalyst. Advances in Natural Sciences: Nanoscience and Nanotechnology. 2017;8(2):025017.

[22] Bouafia A, Laouini SE, Khelef A, Tedjani ML, Guemari F. Effect of ferric chloride concentration on the type of magnetite (Fe_3O_4) nanoparticles biosynthesized by aqueous leaves extract of artemisia and assessment of their antioxidant activities. Journal of Cluster Science. 2021;32(4):1033-41.

[23] Yadav A, Raghav S, Jangid NK, Srivastava A, Jadoun S, Srivastava M, et al. Myrica esculenta leaf extract—assisted green synthesis of porous magnetic chitosan composites for fast removal of Cd (II) from water: Kinetics and thermodynamics of adsorption. Polymers. 2023;15(21):4339.

[24] Kouhbanani MAJ, Beheshtkhoo N, Taghizadeh S, Amani AM, Alimardani V. One-step green synthesis and characterization of iron oxide nanoparticles using aqueous leaf extract of Teucrium polium and their catalytic application in dye degradation. Advances in Natural Sciences: Nanoscience and Nanotechnology. 2019;10(1):015007.

[25] Tabassum R, Dilshad E. A comparative anticancer analysis of iron oxide nanoparticles of Hippophae rhamnoides and Cichorium intybus found in the Karakoram Range of Gilgit Baltistan against liver cancer targeting the RhoA gene. Drug Development and Industrial Pharmacy. 2025;51(9):1078-87.

[26] Yadav VK, Ali D, Khan SH, Gnanamoorthy G, Choudhary N, Yadav KK, et al. Synthesis and characterization of amorphous iron oxide nanoparticles by the sonochemical method and their application for the remediation of heavy metals from wastewater. Nanomaterials. 2020;10(8):1551.

[27] Chiban M, Zerbet M, Carja G, Sinan F. Application of low-cost adsorbents for arsenic removal: A review. J Environ Chem Ecotoxicol. 2012;4(5):91-102.

[28] Joshi S, Sharma M, Kumari A, Shrestha S, Shrestha B. Arsenic removal from water by adsorption onto iron oxide/nano-porous carbon magnetic composite. Applied Sciences. 2019;9(18):3732.

[29] Janjaroen D, Dilokdumkeng P, Jhandrta P. Effect of water hardness and pH on adsorption kinetic of arsenate on iron oxide. Engineering Journal. 2018;22(2):13-23.

[30] Tang W, Li Q, Gao S, Shang JK. Arsenic (III, V) removal from aqueous solution by ultrafine α-Fe2O3 nanoparticles synthesized from solvent thermal method. Journal of Hazardous Materials. 2011;192(1):131-8.

[31] Kamsonlian S, Suresh S, Majumder CB, Chand S. Biosorption of arsenic by mosambi (Citrus limetta) peel: equilibrium, kinetics, thermodynamics and desorption study. Asian Journal of Chemistry. 2013;25(5):2409.

[32] Hall KR, Eagleton LC, Acrivos A, Vermeulen T. Pore-and solid-diffusion kinetics in fixed-bed adsorption under constant-pattern conditions. Industrial & Engineering Chemistry Fundamentals. 1966;5(2):212-23.

[33] Rahdar S, Taghavi M, Khaksefidi R, Ahmadi S. Adsorption of arsenic (V) from aqueous solution using modified saxaul ash: isotherm and thermodynamic study. Applied Water Science. 2019;9(4):87.

[34] Lunge S, Singh S, Sinha A. Magnetic iron oxide (Fe_3O_4) nanoparticles from tea waste for arsenic removal. Journal of Magnetism and Magnetic Materials. 2014;356:21-31.

[35] Ghimire KN, Inoue K, Makino K, Miyajima T. Adsorptive removal of arsenic using orange juice residue. Separation Science and Technology. 2002;37(12):2785-99.

[36] Gyawali D, Rijal S, Basnet P, Ghimire KN, Pokhrel MR, Paudyal H. Effective biosorption of As (V) from polluted water using Fe (III)-modified Pomelo (Citrus maxima) peel: A batch, column, and thermodynamic study. Heliyon. 2023;9(2).